JOINT INSTITUTE FOR NUCLEAR RESEARCH
Bogoliubov laboratory of Theoretical Physics (BLTP)

FINAL REPORT ON THE START PROGRAMME

Isomeric and low-lying excited states of superheavy isotopes

Supervisor:
Prof. Nikolai Antonenko

Student:
Amira Nasr, Egypt
Cairo University

Participation period:
July 21 – September 14,
Summer Session 2024

Dubna, 2024

Abstract

The observation of a rotational band in a nucleus' spectra is the most straightforward method of verifying deformation of a nucleus. The rotational state is the only possibility that can occur if the energy of such a state is discovered to be of about 40–50 keV, as is predicted. Rotational energy E_{I^+} in the I^+ state, is related to the moment of inertia $\mathcal{J}$. The cranking approximation is used to estimate a moment of inertia of a nucleus. Shell structure of deformed superheavy nuclei is significantly reflected in their rotational properties.

We employ the self-consistent mean-field approach in our calculations. The Skyrme-Hartree-Fock-Bogoliubov (HFB) theory is a purely microscopic theory. The study of low-energy nuclear excitations along the α-Decay Chains of the heaviest nuclei presents a challenge to nuclear theory from a theoretical perspective, and it is an extremely challenging task to study these heaviest nuclei experimentally.

Project goals

- To investigate the ground, excited, and isomeric-state masses and energies, and deformations of superheavy isotopes of the atomic number larger than 100.
- To study the characteristics of the potential energy surface (PES) of the presented nuclei.
- To produce the available experimental data.

Scope of work

In this study, we present an extensive study of nuclear structure and explore the properties of isomeric and excited states of super-heavy elements with atomic numbers beyond 100 up to 120 for a wide range of nuclei with N = 148 to 192.

Key Goals:

- Masses and Energies: Calculate ground, excited, and isomeric-state masses and energies.
- Nuclear Deformations: Investigate deformations corresponding to proposed isotopic states.
- Shell closures: predicted the shell closures for protons and neutrons in Skyrme HFB calculations.
- Potential energy surface (PES): qualitatively explain the range of spontaneous fission half-lives observed experimentally and calculate the fission barrier for superheavy nuclei.

Introduction

The observation of a rotational band in a nucleus' spectra is the most straightforward method of verifying deformation of a nucleus. The mainly calculations of the equilibrium deformations, energies of the first 2^+ states, and the probabilities and observation of $\boldsymbol{\alpha}$-decay to the first rotational state 2^+, in addition to electron transitions, presents to be the more promising way to measure the energy of this state for even-even heaviest nuclei in the deformed region. The rotational state is the only possibility that can occur if the energy of such a state is discovered to be of about 40–50 keV, as is predicted. Equilibrium deformation of a nucleus is calculated by minimization of its energy in a multidimensional deformation space. The seven-dimensional space β_λ, $\lambda = 2,3,\dots,8$ is taken. where, β_λ are the usual deformation parameters. In calculations of moment of inertia of nuclei and to describe the rotational energies, it's important to use a multidimensional deformation space, particularly for heaviest nuclei. There is main role of deformations of various multipolarities in the moment of inertia and thus in E_{2+}. When used a multidimensional deformation space the value of the rotational energy decreased.

The rotational energy E_{I+} in the I^+ state, is related to the moment of inertia $\mathcal{J}$. The cranking approximation is used to estimate a moment of inertia of a nucleus. This method provides a good description of the ground-state moments of inertia of well-deformed nuclei as well as a very good description of the energy of the lowest rotational states of even-even heaviest nuclei, particularly those that are the heaviest or most strongly deformed, as fission isomers are. Through the weakening of pairing correlations, to which moments of inertia are highly sensitive, the energy gaps (closed shells or subshells) affect the values of moments of inertia and consequently of the first excited state E_{2+} of nuclei [1]. Shell structure of deformed superheavy nuclei is significantly reflected in their rotational properties. In particular, nuclei with closed deformed shells have the lowest rotational energy $E_{2+}$and the moment of inertia is highest (i.e., moving in the direction to its rigid body limit) where the mechanism is that pairing correlations are weakened at closed shells. For an exact description of rotational energies (moments of inertia) of the heaviest nuclei, a sufficiently large deformation space is required. In order to identify shell or subshell closures in the SHN region, the excitation energy $E_{2+}$of the first excited 2^+ states, is used for this purpose. The study of low-energy nuclear excitations along the α-Decay Chains of the heaviest nuclei presents a challenge to nuclear theory from a theoretical perspective, and it is an extremely challenging task to study these heaviest nuclei experimentally. A lot of effort is currently being put into this showcase of nuclear physics research. Advanced experimental techniques have already made it possible to discover the first nuclear structure information beyond the global properties such as α-decay half-lives and Q_α-values [2,3]. Specialized new facilities in the future are expected to enable the development of more detailed investigations of the nuclear structure for the already synthesized isotopes, in addition to facilitating the search for new elements with even higher Z.

The properties of the SHEs have been examined in a variety of nuclear models simultaneously with the experimental efforts made in the experimental improvements. It is extremely challenging for any theoretical model to accurately describe of trans-fermium nuclei. Nowadays, nuclear physics is very interested in the structure and stability of these nuclei. The main reason for the existence and stability of these heaviest nuclei is achieved by the shell effects. The synthesis of superheavy nuclei (SHN) is progressing rapidly. It has been theoretically predicted that these nuclei will have two regions: one around the spherical doubly magic nucleus $^{298}_{114}Fl$ and the other around deformed nuclei with Z=108–110 and N=162–164. Based on a thorough examination of the ground-state energy and single-particle spectra of these nuclei in a multidimensional deformation space [4], it has been determined that $^{270}_{108}Hs$ represents a doubly magic deformed nucleus. Compared to spherical SHN, the region of deformed SHN seems to be closer to experimentally investigated nuclei and the nuclei that are close to its center ($^{270}_{108}Hs$) were also easier to reach them easily from other nuclei. Therefore, one approach to solving the issue of experimental confirmation of deformed shapes of superheavy nuclei located in the neighborhood of $^{270}_{108}Hs$ is the measurement of the energy E_{2^+} of the lowest 2^+ state in even-even species of the nuclei. For superheavy nuclei, however, the probability of observing such a band is limited due to the extremely low cross sections required for their synthesis. We are interested in confirming our calculations for nuclei for which these energies have been observed before estimating the rotational energies E_{2^+} for superheavy nuclei. Currently, $^{254,256}_{100}Fm$ [5] is the heaviest nuclei for which such bands have been detected, and very recently, $^{252,254}_{102}No$ [6] has also been observed to have a rotational band. The detection of two near lines in the $\boldsymbol{\alpha}$-decay spectrum of $^{260}_{106}Sg$ [7] provided an indication of the energy of the lowest rotational state 2^+ for deformation of the nucleus $^{256}_{104}Rf$ [8].

We employ the self-consistent mean-field approach in our calculations. The Skyrme-Hartree-Fock-Bogoliubov (HFB) theory is a purely microscopic theory that is an ideal tool for the analysis of and provides an improved estimation of the Q-values of α-decay, the predominant decay mode of SHEs, in many cases [9]. Furthermore, all possible shapes of a nucleus are considered in the minimization process in the self-consistent calculations. We present results for the heavier even-even nuclei around the region of the well-known fermium (Fm, Z = 100) up to SHEs and include this region of the (Fm, Z = 100) element in our analysis to compare our predictions with the available experimental data. These nuclei currently reside at the center of the spotlight for SHE experiments. The principal motivation behind these investigations is to provide reliable experimental anchor points for nuclear structure theory in the heavy and superheavy nuclei, as well as to obtain a way to decay schemes that are significant to nuclear structure physics. where the experiment does not clearly show whether the decay occurs between the ground states of the parent and daughter nuclei. As a result, estimating the first excited states E_{2^+} of the two participating nuclei is crucial. Knowing an approximate analysis of the spectra of both nuclei involved in the α-decay could be beneficial in the interpretation of the experimental data. We are excited to investigate the isomeric and low-lying excited states of heavy and superheavy isotopes in order to contribute to the knowledge of the spectra of these isotopes.

Figures

Fig. (1.a)

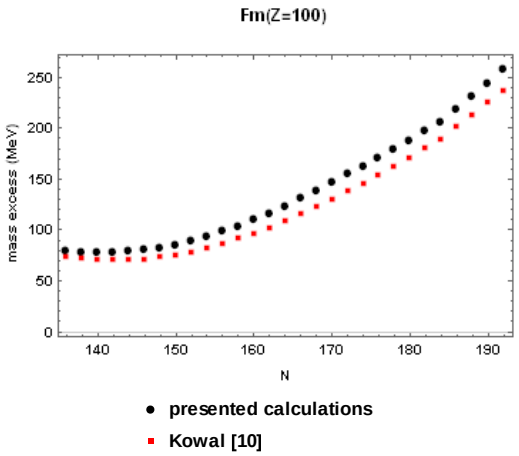

Fig. (1.b)

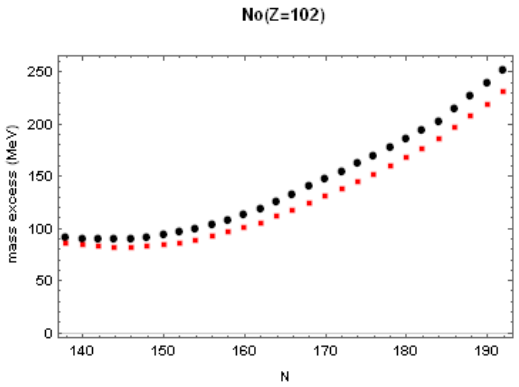

Fig. (1.c)

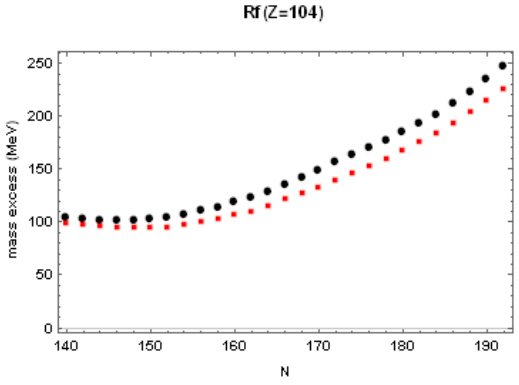

Fig. (1.d)

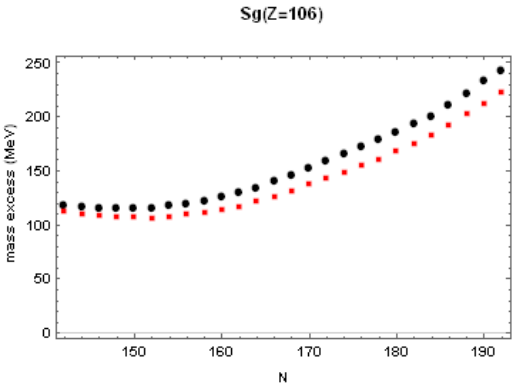

Fig. (1.e)

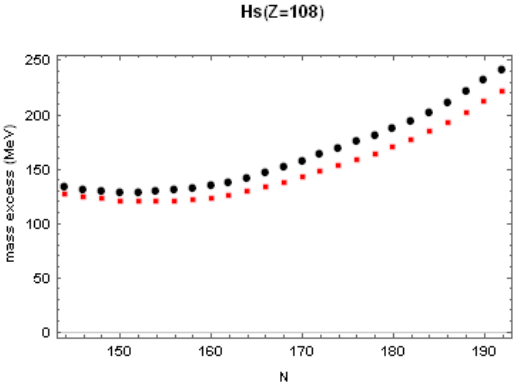

Fig. (1.f)

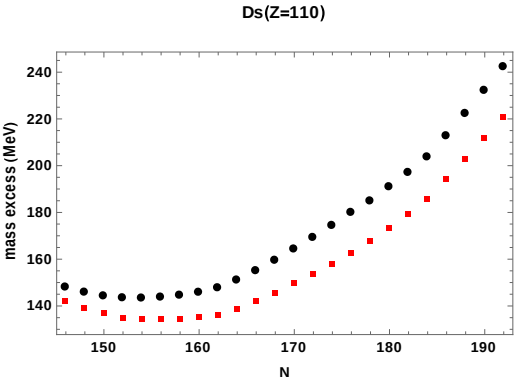

Figures

Fig. (1.g)

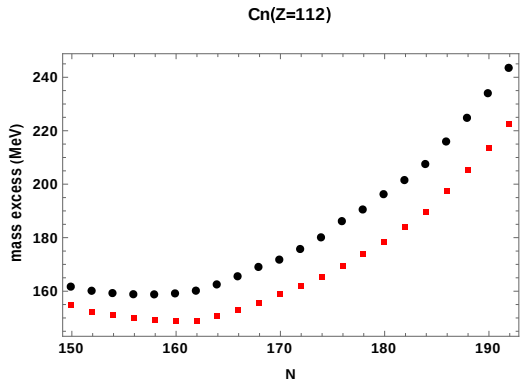

Fig. (1.h)

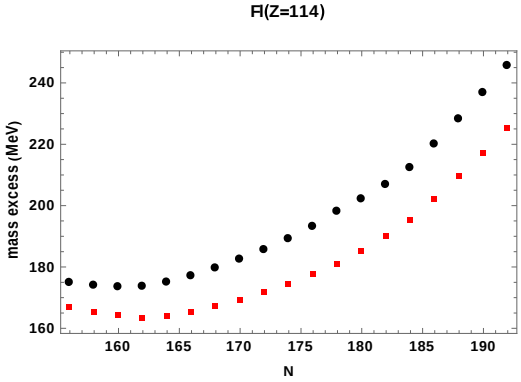

Fig. (1.i)

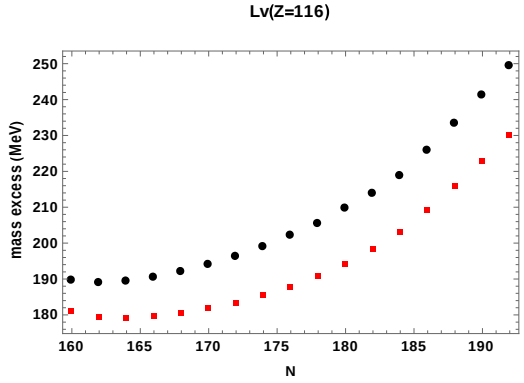

Fig. (1.j)

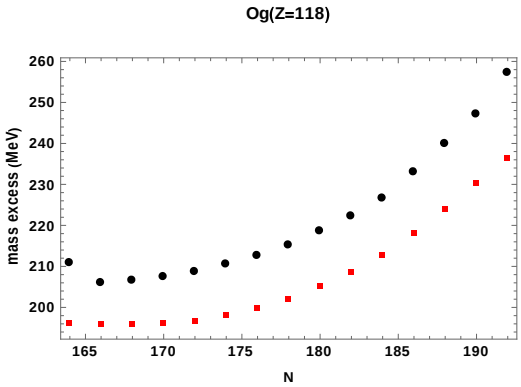

Fig. (1.k)

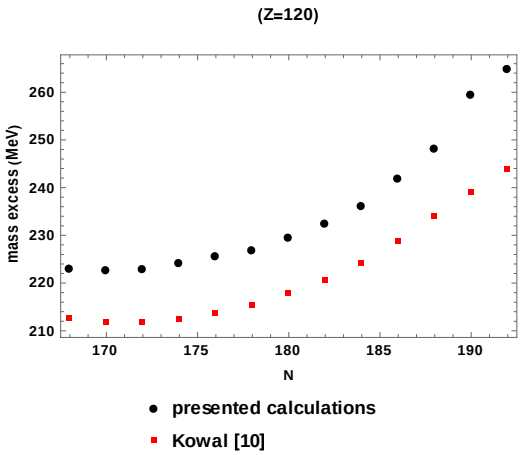

Fig. (1): The mass excess as a function of the neutron number (N) for: (a) $Fm_{126-230}$ (b) $No_{130-236}$ (c) $Rf_{134-234}$ (d) $Sg_{138-232}$ (e) $Hs_{142-230}$ (f) $Ds_{146-228}$ (g) $Cn_{150-226}$ (h) $Fl_{156-224}$ (i) $Lv_{160-222}$ (j) $Og_{164-220}$ (k) $120_{168-218}$.

Figures

Fig. (2.a)

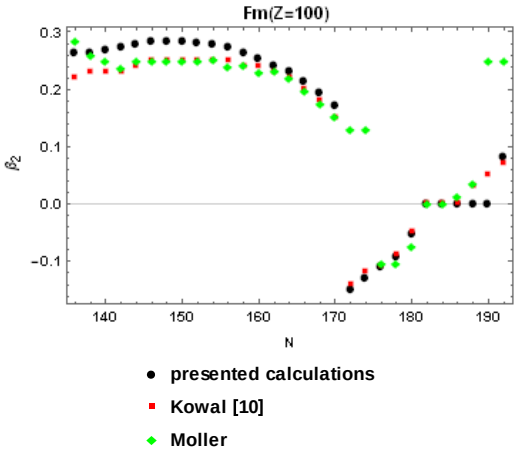

Fig. (2.b)

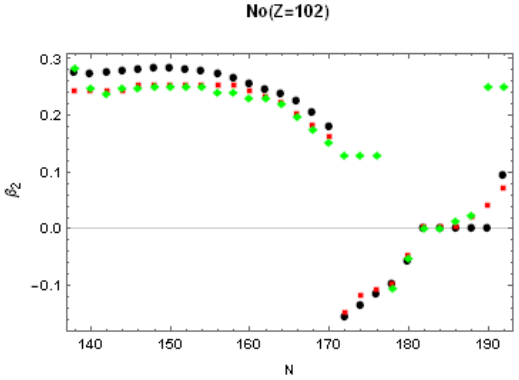

Fig. (2.c)

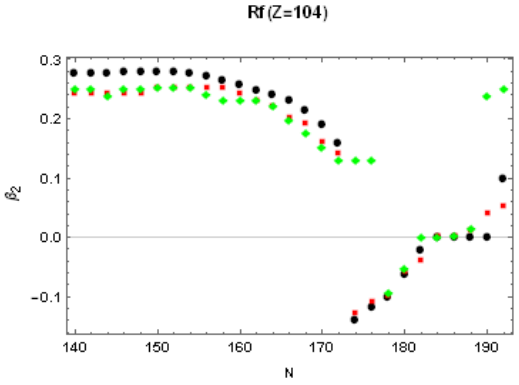

Fig. (2.d)

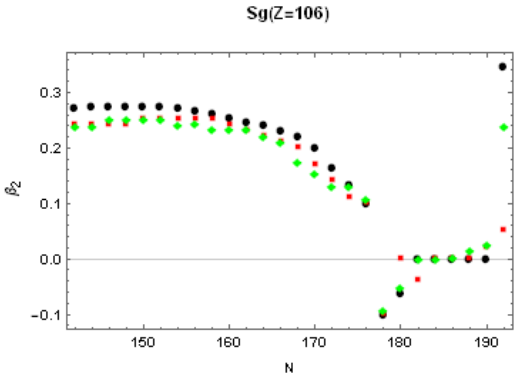

Fig. (2.e)

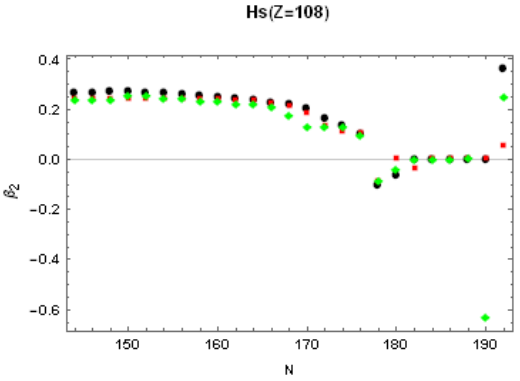

Fig. (2.f)

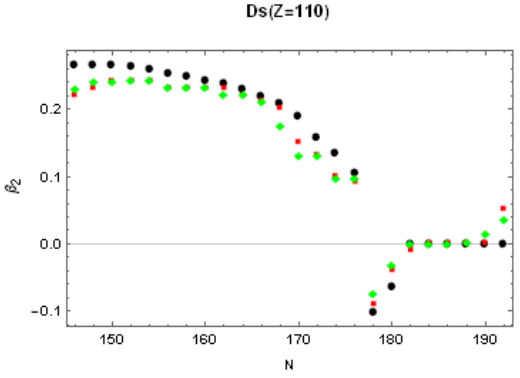

Figures

Fig. (2.g)

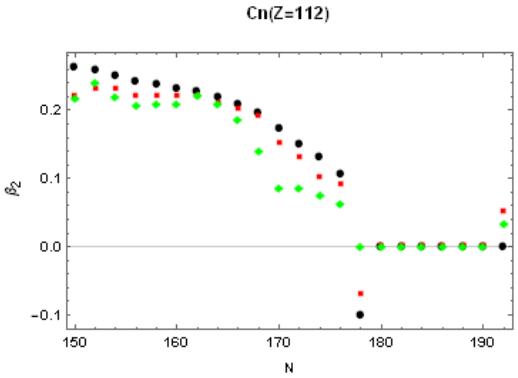

Fig. (2.j)

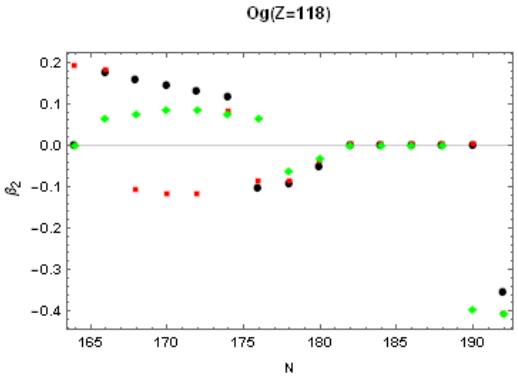

Fig. (2.h)

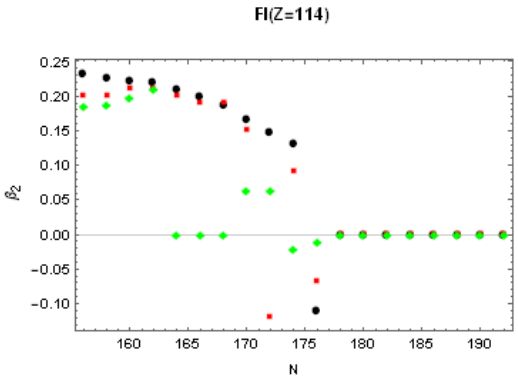

Fig. (2.k)

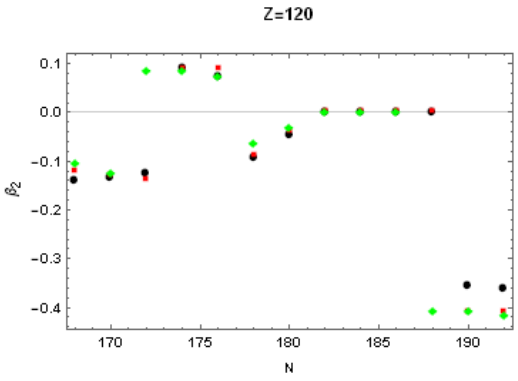

Fig. (2.i)

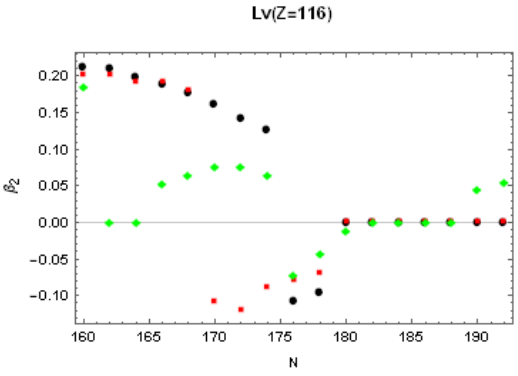

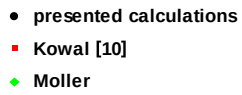

Fig. (2): The quadrupole deformation β_2 as a function of the neutron number (N) for: (a) $Fm_{126-230}$ (b) $No_{130-236}$ (c) $Rf_{134-234}$ (d) $Sg_{138-232}$ (e) $Hs_{142-230}$ (f) $Ds_{146-228}$ (g) $Cn_{150-226}$ (h) $Fl_{156-224}$ (i) $Lv_{160-222}$ (j) $Og_{164-220}$ (k) $120_{168-218}$.

Figures

Fig. (3.a)

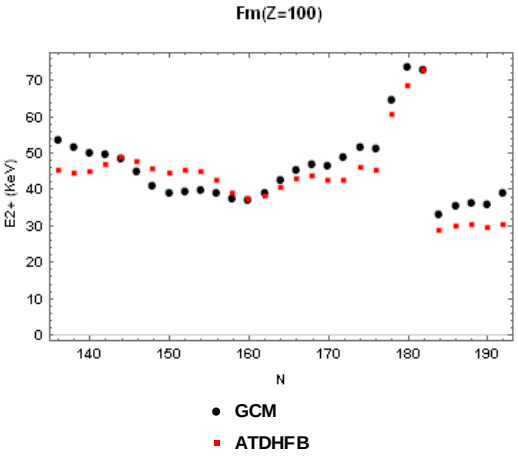

Fig. (3.b)

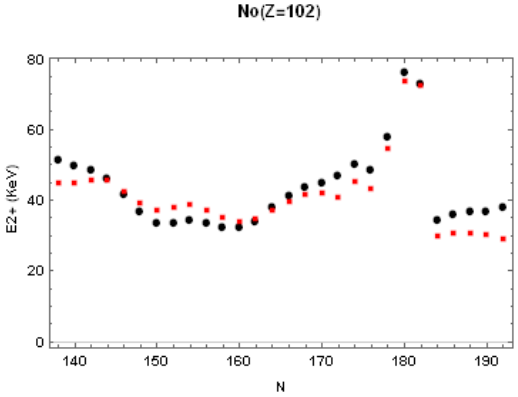

Fig. (3.c)

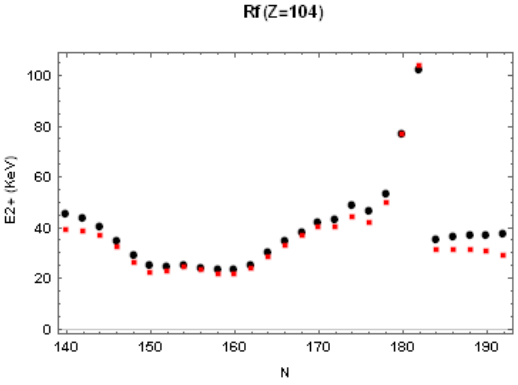

Fig. (3.d)

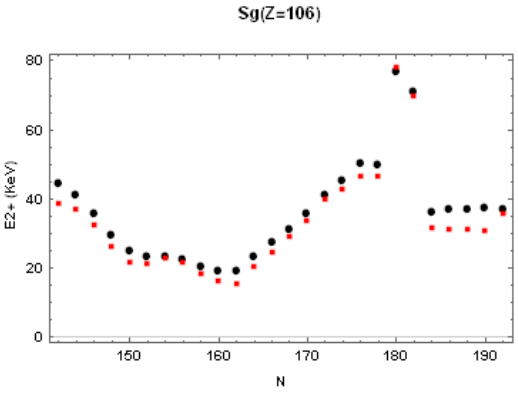

Fig. (3.e)

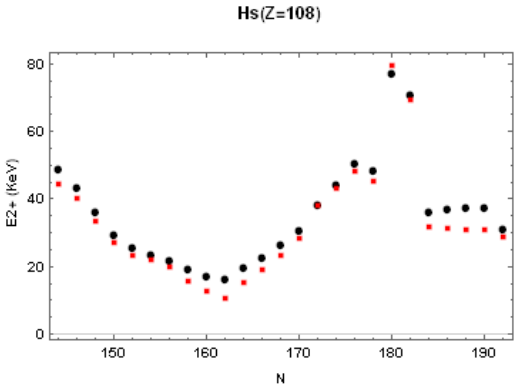

Fig. (3.f)

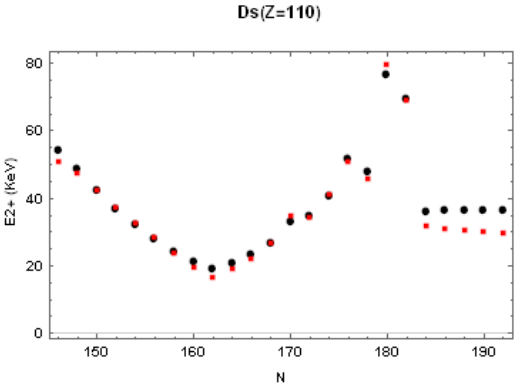

Figures

Fig. (3.g)

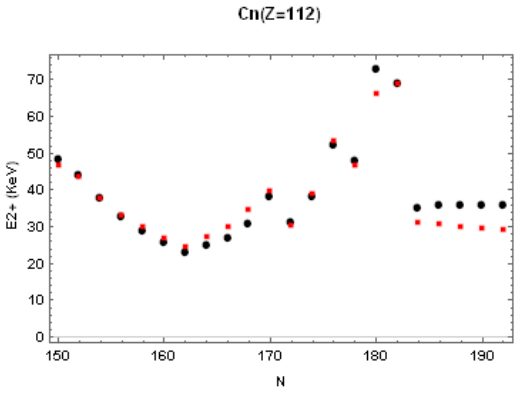

Fig. (3.h)

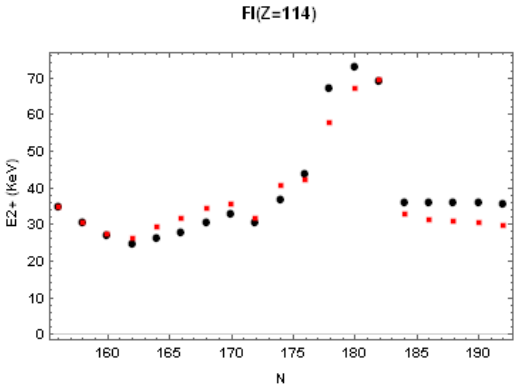

Fig. (3.i)

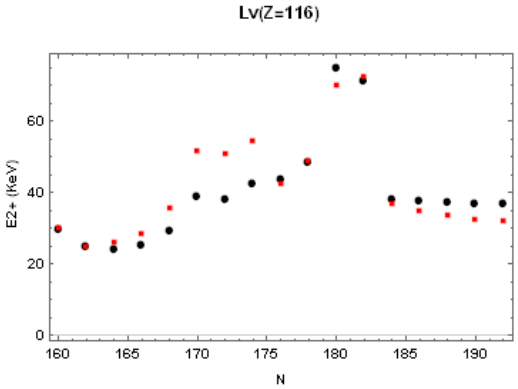

Fig. (3.j)

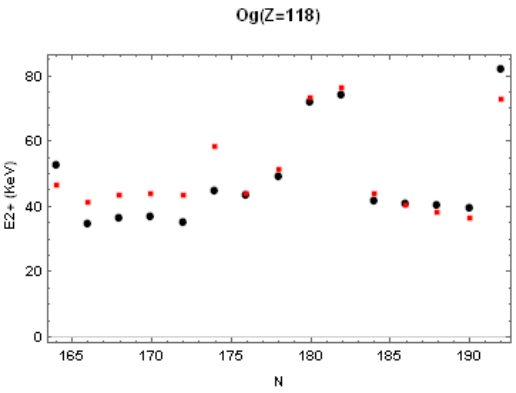

Fig. (3.k)

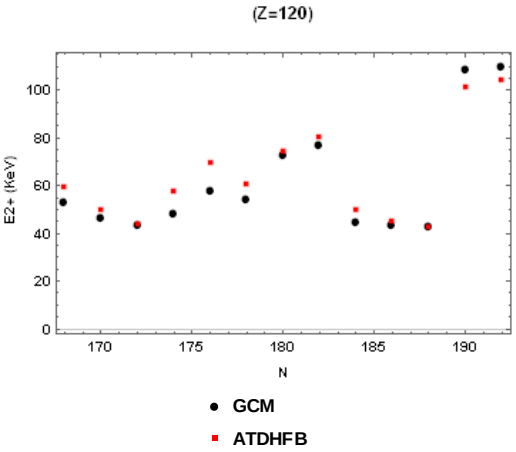

Fig. (3): The energy $E_{2+}$of the first rotational state 2+ as a function of the neutron number (N) for: (a) $\mathrm{Fm}_{126-230}$ (b) $\mathrm{No}_{130-236}$ (c) $\mathrm{Rf}_{134-234}$ (d) $\mathrm{Sg}_{138-232}$ (e) $\mathrm{Hs}_{142-230}$ (f) $\mathrm{Ds}_{146-228}$ (g) $\mathrm{Cn}_{150-226}$ (h) $\mathrm{Fl}_{156-224}$ (i) $\mathrm{Lv}_{160-222}$ (j) $\mathrm{Og}_{164-220}$ (k) $120_{168-218}$.

Figures

Fig. (4.a)

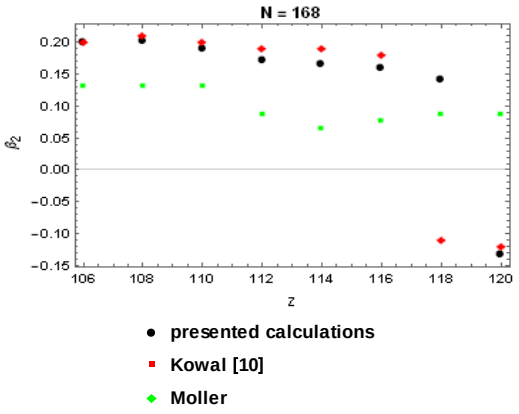

Fig. (4.b)

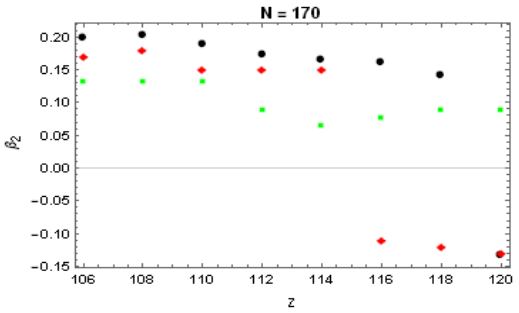

Fig. (4.c)

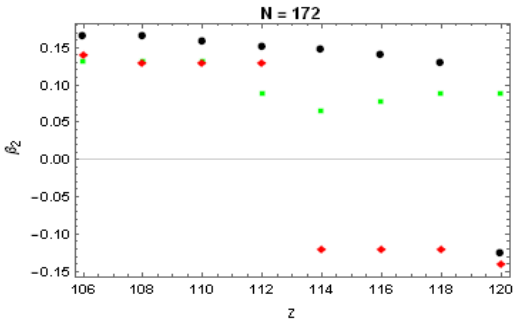

Fig. (4.d)

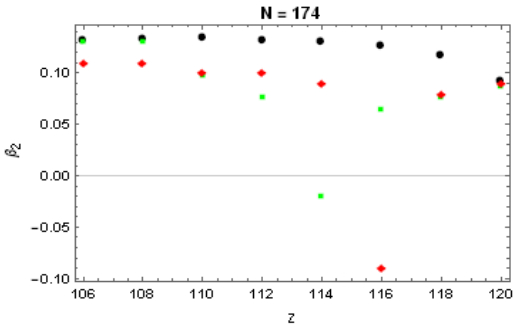

Fig. (4.e)

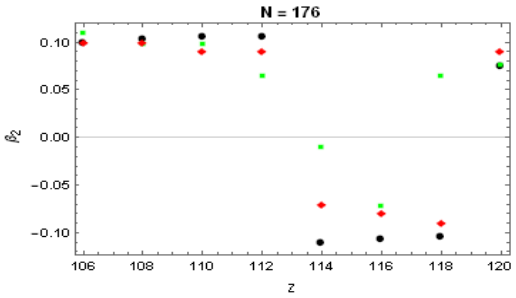

Fig. (4.f)

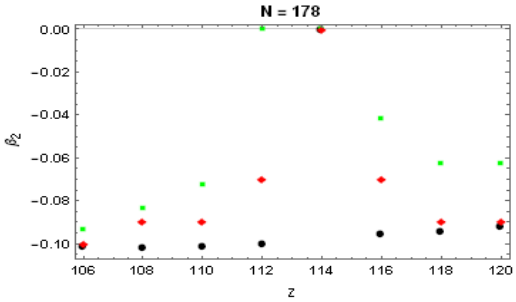

Fig. (4.g)

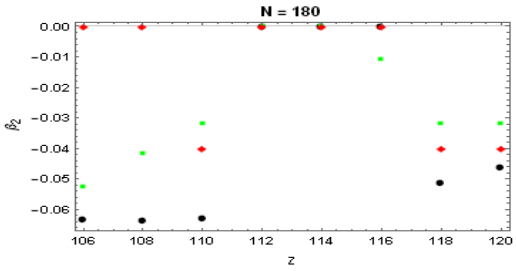

Fig. (4.h)

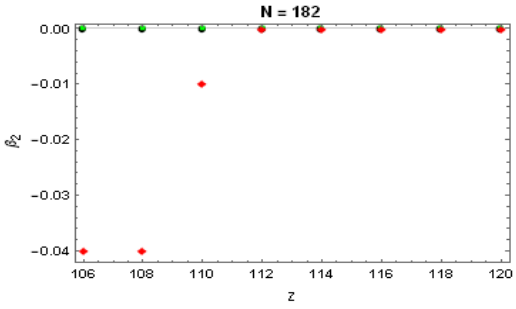

Fig. (4): The quadrupole deformation β_2 as a function of the atomic number (Z) at constant neutron number for: (a) N = 168 (b) N = 170 (c) N = 172 (d) N = 174 (e) N = 176 (f) N = 178 (g) N = 180 (h) N = 182.

Figures

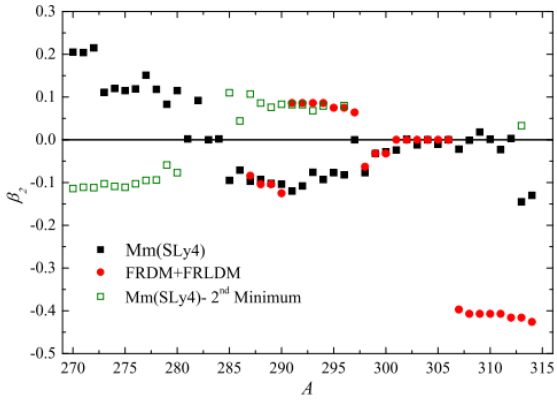

Fig. (5): The quadrupole deformation parameter (.β_2), obtained from the present Mm(SLy4), for $270-314_{120}$ isotopes as functions of mass number (A). The results based on the FRDM and FRLDM [11] calculations are added for comparison. Open green squares in panel (b) Represent β_2 values for the second lowest minima in the total energy surface obtained from Mm(SLy4) calculations.

Discussion

Figures 1 (a-k) show the mass excess as a function of neutron number (N) for isotopes of Z = 100 to Z = 120. Figure (1) also displays the corresponding values of mass excess as calculated using the Skyrme Hartree-Fock-Bogoliubov (HFB) theory, which is a purely microscopic theory as the self-consistent mean-field approach, and the calculations of Kowal are based on microscopic-macroscopic method with the deformed Woods–Saxon single-particle potential and the Yukawa-plus-exponential macroscopic energy taken as the smooth part., for comparison. It's evident in fig. (1.a) that the two methods agree in estimating the mass excess in terms of the general trend of variation with neutron number (N) and, of course, also agree in estimating the total binding energy. For all Z = 100-120, It's noticeable that the relative differences between the values of mass excess. deduced from the two methods increase with increasing the neutron number (N). The calculations of the present Skyrme HFB calculations estimate a little larger mass excess relative to the microscopic-macroscopic method (Kowal) calculations.

In addition to the values of β_2 corresponding to the lowest minima of total energy of the investigated isotopes according to the Skyrme Hartree-Fock-Bogoliubov (HFB), microscopic-macroscopic (Kowal), and FRDM (M*ö*ller) methods, we add in figures 2(a-k). The predictions three calculations for β_2 are consistent for isotopes of Z = 100 to 120. Also, the shapes of the nuclei, whether spherical ($\beta_2 = 0$), prolate ($\beta_2 > 0$), or oblate ($\beta_2 < 0$). We noticed that mostly the isotopes have prolate shapes, and there are five even-even isotopes for Z = 100-104, 120 and two or three even-even isotopes for Z = 106-110, 116,118, and just one even-even isotope for Z = 112, 114 oblate shapes.

In most isotopes of Z = 100-120, there is agreement in the predictions of Skyrme HFB calculations, microscopic-macroscopic (Kowal), and FRDM (M*ö*ller) calculations for β_2. while there are regions of agreement between the three methods in Z = 100-106, 110-112, and 116, but in contrast, the nuclei with N = 188, 190 have spherical shapes predicted by Skyrme HFB calculations, and they show prolate nuclear shapes based on microscopic-macroscopic (Kowal), and FRDM (M*ö*ller) calculations. But these 306_{Lv}, 308_{Og} isotopes show spherical shapes also in calculations of microscopic-macroscopic (Kowal). Also, in contrast to the oblate shapes predicted by Skyrme HFB and microscopic-macroscopic (Kowal) calculations for these $272, 274_{Fm}$, $274,276,278_{No}$, $278,280_{Rf}$ isotopes, they show prolate shapes based on the FRDM (M*ö*ller). In these 292_{Fm}, 294_{No}, 296_{Rf} isotopes the value of β_2 in M*ä*ller calculation is more prolate than in the Skyrme HFB and microscopic-macroscopic (Kowal) calculations. And also, in contrast to the spherical shape predicted by Skyrme HFB and microscopic-macroscopic (Kowal) calculations for this 298_{Hs} isotope, it has an oblate shape based on FRDM (M*ö*ller) calculations. And this 290_{Cn} isotope has a spherical shape in FRDM (M*ö*ller) calculations, in contrast to the oblate shape predicted by Skyrme HFB and microscopic-macroscopic (Kowal) calculations. In most isotopes of Z = 114, 116 and 118, there is agreement in the predictions of Skyrme HFB calculations, and microscopic-macroscopic (Kowal) calculations for β_2. But these 286_{Fl} $286, 288, 290_{Lv}$ $286, 288, 280_{Og}$, isotopes have a prolate shape in Skyrme HFB and FRDM (M*ö*ller) calculations, in contrast to the oblate shape predicted by microscopic-macroscopic (Kowal) calculations. In all

isotopes of Z = 120 there is agreement in the predictions of three methods, but this 308_{120} isotope shows spherical nuclear shapes based on Skyrme HFB and microscopic-macroscopic (Kowal) in contrast to the oblate shape predicted by FRDM (Möller) calculations. Also, we noticed that the switch in shape from prolate to oblate nuclear shape can occur at N = 170, 172, 176, 174 of the isotopes of Z = 100-102, 104, 106-112, 114-118, respectively.

The energy E_{2+} of the first rotational state 2+ as a function of the neutron number (N) calculated for a wide region of nuclei with Z = 100-120 and N = 140-192 using the Skyrme Hartree-Fock-Bogoliubov (HFB) theory is shown in figure (4). Figures 4(a-k) also show the calculations from two different methods using to calculate the ground-state moments of inertia then calculate the energy E_{2+} of the first rotational state 2+, the two methods are generator coordinate method (GCM) and adiabatic time-dependent Hartree-Fock-Bogolyubov (ATDHFB) approximation. In the case of GCM, the calculation is performed using the local approximation of the Gaussian overlap approximation (GOA), while in case of the ATDHFB theory, we use the perturbative cranking approximation. One can see those two minima of E_{2+} are obtained for the considered nuclei corresponding to N = 152, and 162. The more important reason for these minima is the exceptional shell structure of the nuclei studied, or more particularly, the appearance of strong deformed shells closed at N =162 and weaker shell closed at N = 152. Because the energy gaps (closed shells or subshells) influence the values of moments of inertia and thus of E_{2+} of nuclei so, the shell closures at N = 152 and 162 leads to large values of the moment of inertia and this way to small values of E_{2+}. And we can see clearly, in figures (4) the dependence of E_{2+} on neutron number N around the shell closures at N = 152 and 162. Also, we noticed that at the neutron number N = 184, the values of E_{2+} are very large where N = 184 is spherical shell closure.

Figures 4(a-h) show β_2 corresponding to the lowest minima of total energy of the investigated isotopes according to the Skyrme Hartree-Fock-Bogoliubov (HFB), microscopic-macroscopic (Kowal), and FRDM (Mäller) methods as a function of proton number (Z) at constant neutron number (N = 168, 170, 172, 174, 176, 178, 180, and 182). We added these figures to illustrate the shell closure for protons and neutrons. We observed clearly that, for neutrons, N = 184 and 182 are spherical shell closure, and for protons, Z = 114 maybe is spherical shell closure also and it has appeared in figures 4(f-h).

We can focus on quadrupole deformation beta for Z = 120 and give a comparison between our presented calculations based on Skyrme HFB calculations and our calculations in my MSC [12] based on the macro-micro model, is shown in figure (5). In addition to the values of β_2 corresponding to the main lowest minima of the ground state energy of the investigated isotopes according to the Mm(SLy4) and FRDM methods of calculation, we add in Fig.(5), the values of β_2 (open green squares) corresponding to the second lowest minima in the total energy surface based on the present Mm(SLy4) calculations, when appeared. The total energy difference between the first and second minima for the modes presented in Fig. (5) is less than 4.0 MeV, which is averagely less than 0.02% of the total energy and less than 0.015MeV of the corresponding energy per nucleon. The Mm (SLy4) calculations predict the $270 - 280, 282_{120}$ isotopes to be of prolate shape, and the three $281,283,284_{120}$ to be spherical. The heavier Z = 120 isotopes turn out to be of oblate shape (up to A = 299 and A = 313, 314) or again spherical. The range of β_2 is deduced

based on the Mm (SLy4) calculations as $-0.145 \leq \beta_2 \leq 0.215$ throughout the study domain. On the other hand, the FRDM method estimates oblate shape of extreme large negative values of β_2, up to $\beta_2 = -0.426$, for the $307 - 314_{120}$ isotopes. The predictions of the two presented methods for the ground state β_2 deformation are consistent for isotopes with mass numbers A ≤ 290 and A = 298–306. In contrast to the oblate shape predicted by the Mm (SLy4) calculations, the $291 - 296_{120}$ isotopes show prolate nuclear shapes based on the FRDM calculations. It is worth noting that these isotopes that did not show agreement in the ground state β_2 deformation based on the FRDM calculations with that of the Mm (SLy4) calculations show agreement with its β_2 of their second lowest minima. The total energy difference between the two minima for these isotopes is less than 0.5 MeV, except for 295_{120} with a difference of about 8 MeV. The two methods confirm the spherical shape to the isotopes of A = 300–306, around the neutron shell closure of N = 184.

Theory

One of the successful codes that can be used to perform HFB calculations is HFBTHO (V4.0) [13]. The HFB method can be used to predict the structure of nucleus. In this method we can implement the energy density function (EDF) approach to calculate the different properties of atomic nuclei. The energy density function can be derived based on the zero-range Skyrme or the finite-range Gogny effective nucleon interaction, where the energy of the nucleus is obtained by integration over space of some phenomenological energy density, which is itself a functional of the neutron and proton intrinsic densities. The HFBTHO (V4.0) program uses the axial harmonic oscillator (HO) or transformed harmonic oscillator (THO) single-particle basis to expand quasiparticle wave functions. The program can be used in a variety of applications, including systematic studies of wide ranges of nuclei, both spherical and axially deformed, extending all the way out to nucleon drip lines. The inertia tensor that enters the kinetic energy term of the collective Schrödinger-like equation is one of the most essential ingredients of the theory, since it includes the response of the system to small changes in the collective variables. For this reason, the two main approximations used to compute this inertia tensor, the adiabatic time-dependent HFB and the generator coordinate method. Fission can then be viewed as a process during which the deformation becomes so large that two separate fragments appear. This viewpoint can be formalized by introducing a set of collective variables that represent the motion of the nucleus as a whole and control the fission process. The characteristics of the resulting potential energy surface (PES), i.e. the energy as a function of the chosen collective variables, determines fission properties. For example, differences in the characteristics of potential energy barriers of nuclei qualitatively explain the range of spontaneous fission half-lives observed experimentally. In neutron-induced fission, the time ‘from saddle to scission’, which is the time it takes for the nucleus to go from the top of the highest barrier to a configuration with two separated fragments, is also strongly dependent on the characteristics of the PES. In the adiabatic approximation, it is further assumed that there is a perfect decoupling between the motion in collective space and the intrinsic motion of individual nucleons. In a phenomenological picture of fission, the collective inertia B can be introduced when the dynamics is assumed to be restricted to a path in the manifold of collective

variables with the associated classical action. In nuclear physics, the notion of collective inertia also arises naturally in theories of large amplitude collective motion such as the generator coordinate method (GCM) or the adiabatic time-dependent Hartree–Fock–Bogoliubov (ATDHFB) theory. Therefore, these general approaches to the quantum many-body problem provide rigorous methods to compute the collective inertia needed in fission. The collective inertia tensor is a function of the collective variables and depends sensitively on both the shell structure and pairing correlations.

The full description of nuclear density distributions requires the definition of the radial dependence (which describes the size and diffused edge of the distribution), and the angular dependence (which describes the nuclear shape and deformations). For microscopic calculations, density is the sum of single particle densities.

$$\rho_i(\boldsymbol{r}) = \sum_i |\varphi_i(\boldsymbol{r})|^2$$

Index i labels the neutron (i = n) or proton (i = p). The problem of nuclear structure is a many-body problem. Since it's a complicated problem. In the mean-field models, the totality of the interactions acting on a nucleon is an average potential is approximated. In such average potential a nucleon moves independently from the other constituents of the system. These models concentrate on self-consistent determination of the nuclear mean-field (SCMF), i.e., (HF) method and its generalizations (HFB). For this purpose, effective interactions are employed. This concept is closely related to energy-density-functional (EDF) theory in electronic systems. According to this model, nucleons can move in average potential independently from each other, so the problem of the Hartree-Fock method is how to extract a single-particle potential out of the sum of two-body interactions.

$$V(1, \dots., A) = \frac{1}{2}\sum_{i \neq j}^{A} V(r_{i,} r_{j,})$$

Single-particle potential can be derived by a variational principle using the Slater determinants as wave functions. The variational principle solves in approximated way the eigenvalue problem of the exact Schrödinger equation

$$\widehat{H}|\Psi\rangle = E|\Psi\rangle \qquad \text{eq. 1}$$

This approach is useful for solving many-body problems, and it's used not only in Hartree-Fock method, but also in other important theories in nuclear physics like the Bardeen-Cooper-Schrieffier (BCS) theory, for pairing interaction. HF-theory tries to give a microscopic explanation to the existence of a nuclear mean-field. It starts from a many body Hamiltonian which a two-body interaction between nucleons

$$\widehat{H} = \widehat{T} + V = \frac{-h^2}{2m}\sum_i \nabla_i^2 + \frac{1}{2}\sum_{i \neq j} V(i,j) \qquad \textit{eq. 2}$$

The purpose of the HF method is resolving an eigenvalue problem in which the total wave function has the form of the totally anti-symmetric product of single-particle wave functions φ_i, this total wave function is determined by the slater determinant:

$$\Psi(\vec{r}_1, \ldots\ldots, \vec{r}_A) = \frac{1}{\sqrt{A!}} \begin{bmatrix} \varphi_1(\vec{r}_1) & \cdots & \varphi_1(\vec{r}_A) \\ \vdots & \ddots & \vdots \\ \varphi_A(\vec{r}_1) & \cdots & \varphi_A(\vec{r}_A) \end{bmatrix} \qquad \textit{eq. 3}$$

In order to find the minimum of the energy functional, now the variational principle to the eigenvalue problem eq. 1 has to be applied, where the Hamiltonian is expressed in eq. 2. Before applying the variational principle it's important to add a Lagrange multiplier. The solution of the Hartree-Fock equations must be found in an iterative way.

1. One starts by choosing a specific potential (like a Saxon-Woods potential or the harmonic oscillator potential) to be applied to the equation of Schrödinger equation and find a wave function.
2. Then this first wave function has to be put again in the equations of Schrödinger equation.
3. And a new potential will be obtained.
4. Then Hartree-Fock equations can be solved by repeating several times this procedure until convergence.

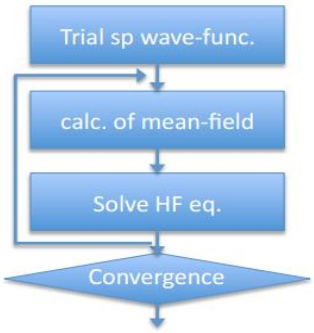

In order to generalize the Hartree-Fock equations, the single-particle wave function can be generalized by making they depend on spin and isospin coordinates

$$\varphi_i(\vec{r}) \rightarrow \varphi_i(\vec{r}, \vec{\sigma}, q_i)$$

Where q stays for the nucleon charge. In the HF approach only take the particle-hole interaction into account, where there is a clear difference between occupied and unoccupied state. This leads to a successful approximation in nuclei with closed shell, but for most nuclei, one also needs to consider the particle-particle or pairing interaction. For these nuclei, the mean field without taking pairing correlations into consideration doesn't perform well. Therefore, the HFB method is introduced to solve this problem for the mean field. Hartree-Fock-Bogolyubov theory generalizes and unifies the simple HF method and the BCS model. The Hamiltonian reduces to two average potentials a self-consistent field, which is known from the pure HF theory and the additional pairing potential, known from the BCS model. The HFB equations constitute a set of non-linear equations to be solved using a self-consistent loop similar to that presented in the case of the HF method. A two-body Hamiltonian of a system of fermions can be expressed in terms of a set of annihilation and creation operators ($c,\ c^{\dagger}$)

$$H = \sum_{n_1 n_2} e_{n_1 n_2} c^{\dagger}_{n_1} c_{n_2} + \frac{1}{4} \sum_{n_1 n_2 n_3 n_4} \bar{v}_{n_1 n_2 n_3 n_4} c^{\dagger}_{n_1} c^{\dagger}_{n_2} c_{n_4} c_{n_3} \quad \text{eq. 4}$$

Where $e_{n_1 n_2}$ and $\bar{v}_{n_1 n_2 n_3 n_4}$ are matrix elements of the kinetic energy operator and anti-symmetrized two-body interaction matrix elements, respectively. The basis of HFB method is the concept of Bogolyubov quasi-particles, that are defined through the so called Bogolyubov transformation. In the HFB method, the ground-state wave function $|\Phi\rangle$ is defined as the quasiparticle vacuum $\alpha_k |\Phi\rangle = 0$, where the quasiparticle operators $(\alpha,\ \alpha^{\dagger})$ are connected to the original particle operators via linear Bogolyubov transformation,

$$\alpha_k = \sum_n \left(U^*_{nk} c_n + V^*_{nk} c^{\dagger}_n \right), \qquad \alpha^{\dagger}_k = \sum_n \left(V_{nk} c_n + U_{nk} c^{\dagger}_n \right)$$

Where U_{nk} and V_{nk} are two transformation matrices. The indices (k) is run over the whole configuration space. Which can be rewritten in the matrix form as

$$\begin{pmatrix} \alpha \\ \alpha^{\dagger} \end{pmatrix} = \begin{pmatrix} U^{\dagger} & V^{\dagger} \\ V^T & U^T \end{pmatrix} \begin{pmatrix} c \\ c^{\dagger} \end{pmatrix}$$

Where $U\ and\ V$ are the coefficients that transform the single-particle states (i) into quasiparticle state (n). In terms of the normal ρ and pairing $\tilde{\rho}$ one-body density matrices, defined as

$$\rho_{nn'} = \left\langle \Phi | c^{\dagger}_{n'} c_n | \Phi \right\rangle = (V^* V^T)_{nn'} \qquad , \tilde{\rho}_{nn'} = \left\langle \Phi | c_{n'} c_n | \Phi \right\rangle = (V^* U^T)_{nn'}$$

The expectation value of the Hamiltonian eq. 4 is expressed as an energy functional

$$E[\rho,\ k] = \frac{\langle \Phi | H | \Phi \rangle}{\langle \Phi | \Phi \rangle} \quad \text{eq. 5}$$

The single particle-hole (Hartree-Fock (Γ)) and particle-particle (pairing (Δ)) mean-fields have to be computed from $(\rho\ and\ \tilde{\rho})$ and quasi-particle Hamiltonian matrix H can be diagonalized and the resulting eigenvectors are used as inputs for the subsequent iteration. Variation of energy eq. 5 with respect to $(\rho\ and\ \tilde{\rho})$ results in the HFB equations

$$\begin{pmatrix} e + \Gamma - \lambda & \Delta \\ -\Delta^* & -(e + \Gamma)^* + \lambda \end{pmatrix} \begin{pmatrix} U \\ V \end{pmatrix} = E \begin{pmatrix} U \\ V \end{pmatrix} \quad \text{eq. 6}$$

Where the Lagrange multiplier λ has been introduced to fix the correct average particle number. Nuclear density functional theory (DFT) is one of the most reliable methods for calculating properties of nuclei within the whole nuclear mass chart. DFT is based on the idea that there exists a universal nuclear energy density functional (UNEDF) which represents the total energy of the system as a functional $E[\rho, \tilde{\rho}]$, of the normal ρ and pairing $\tilde{\rho}$ one-body density matrices. Initially, attempts to build a UNEDF were rooted in the zero-range Skyrme interaction treated within the HF or HFB approximation. For Skyrme forces, the HFB energy has the form of a local energy density functional, the energy is expressed as the integral of energy density functional,

$$E[\rho, \tilde{\rho}] = \int \mathcal{H}(\boldsymbol{r})\, d\boldsymbol{r}\,. \qquad \textit{eq. 7}$$

The energy density functional $\mathcal{H}$ is the sum of the mean-field and pairing energy densities,

$$\mathcal{H}(\boldsymbol{r}) = H(\boldsymbol{r}) + \tilde{H}(\boldsymbol{r}). \qquad \textit{eq. 8}$$

Where $H(\boldsymbol{r})\ and\ \widetilde{H}(\boldsymbol{r})$ depend on the particle local density $\rho(\boldsymbol{r})$, pairing local density $\tilde{\rho}(\boldsymbol{r})$, kinetic energy density $\tau(\boldsymbol{r})$, and spin-current density $\boldsymbol{J}_{ij}(\boldsymbol{r})$.

Variation of energy eq. 7 with respect to $\rho\ and\ \rho^{`}$(spin-dependent one-body density matrices) results in the Skyrme HFB equations

$$\Sigma_{\sigma^{`}}\begin{pmatrix} h(\boldsymbol{r},\sigma,\sigma^{`}) & \tilde{h}(\boldsymbol{r},\sigma,\sigma^{`}) \\ \tilde{h}(\boldsymbol{r},\sigma,\sigma^{`}) & -h(\boldsymbol{r},\sigma,\sigma^{`}) \end{pmatrix}\begin{pmatrix} U(E,\boldsymbol{r}\sigma^{`}) \\ V(E,\boldsymbol{r}\sigma^{`}) \end{pmatrix} = \begin{pmatrix} E+\lambda & 0 \\ 0 & E-\lambda \end{pmatrix}\begin{pmatrix} U(E,\boldsymbol{r}\sigma) \\ V(E,\boldsymbol{r}\sigma) \end{pmatrix} \qquad \text{eq. 9}$$

In the present implementation, we make the restriction to Axially-symmetric, Time-reversal-symmetric, and Reflection-symmetric shapes in order to obtain HFB solutions within a much shorter CPU time. Therefore, quasi-particle HFB states can be written in the following form

$$\begin{pmatrix} U_k(\boldsymbol{r},\sigma,\tau) \\ V_k(\boldsymbol{r},\sigma,\tau) \end{pmatrix} = \chi_{qk}(\tau)[\begin{pmatrix} U_k^+(r,z) \\ V_k^+(r,z) \end{pmatrix} e^{i\Lambda^-\varphi}\chi_{+\frac{1}{2}}(\sigma) + \begin{pmatrix} U_k^-(r,z) \\ V_k^-(r,z) \end{pmatrix} e^{i\Lambda^+\varphi}\chi_{-\frac{1}{2}}(\sigma)] \qquad \text{eq. 10}$$

The solution of the HFB eq. 9 is obtained by expanding the quasi-particle function of eq. 10 in a given complete set of basis wave functions that conserve axial symmetry and parity. The program HFBTHO is able to do so far the two basis sets of wave functions (HO and THO). The HO set consists of eigenfunctions of a single-particle Hamiltonian for an axially deformed harmonic oscillator potential. By using the standard oscillator constants

$$\beta_z = \frac{1}{b_z} = (\frac{mw_z}{\hbar})^{1/2}, \qquad \beta_\perp = \frac{1}{b_\perp} = (\frac{mw_\perp}{\hbar})^{1/2}$$

The HO eigenfunctions are written explicitly as

$$\Phi_\alpha(\boldsymbol{r},\ \sigma) = \psi_{n_r}^{\Lambda}(r)\psi_{n_z}(z)\frac{e^{i\Lambda\varphi}}{\sqrt{2\pi}}\chi\Sigma(\sigma) \qquad \text{eq. 11}$$

The set of quantum numbers $\alpha = \{n_r, n_z, \Lambda, \Sigma\}$ includes the numbers of nodes, n_r and n_z, in the r and z directions, respectively and the projections on the z-axis, $\Lambda\ and\ \Sigma$, of the angular momentum operator and the spin. The THO set of basis wave functions consists of transformed harmonic oscillator functions, which are generated by applying the local scale transformation (LST) to the HO single-particle wave functions, which transforms the incorrect Gaussian asymptotic behavior of deformed HO wave functions into the correct exponential form. In the axially deformed case, the LST acts only on the cylindrical coordinates r and z

$$r \to r' \equiv r'(r,\ z) = r\ \frac{f(R)}{R},$$

$$z \to z' \equiv z'(r,\ z) = z\ \frac{f(R)}{R},$$

And the resulting THO wave functions read

$$\Phi_\alpha(\boldsymbol{r},\ \sigma) = \sqrt{\frac{f^2(R)}{R^2}\frac{\partial f(R)}{\partial R}}\psi_{n_r}^{\Lambda}\left(r\ \frac{f(R)}{R}\right)\psi_{n_z}\left(z\ \frac{f(R)}{R}\right)\frac{e^{i\Lambda\varphi}}{\sqrt{2\pi}}\chi\Sigma(\sigma) \qquad \text{eq. 12}$$

Where $R = \sqrt{\frac{z^2}{b_z^2} + \frac{r^2}{b_\perp^2}}$, and $f(R)$ is a scaler LST function.

References:

[1] A. Sobiczewski, Phys. Rev. C 63, 034306 (2001).

[2] D. Rudolph et al., Phys. Rev. Lett. 111, 112502 (2013).

[3] U. Forsberg *et al.,* Nucl. Phys. A953, 117 (2016).

[4] Z. Patyk and A. Sobiczewski, Nucl. Phys. A533, 132 (1991).

[5] Table of Isotopes, 8th ed., edited by R. B. Firestone and V. S. Shirley (Wiley, New York), Vol. 2, (1996).

[6] R. D. Herzberg and M. Leino Eur. Phys. J. A 43, 55–66 (2010)

[7] G. Munzenberg, S. Hofmann, H. Folger, *et al.,* Phys. A 322, 227 (1985).

[8] G. Munzenberg and P. Armbruster, in Exotic Nuclear Spectroscopy, edited by W.C. McHarris (Plenum, New York), p. 181 (1990).

[9] A. Staszczak, A. Baran, and W. Nazarewicz Phys. Rev. C87 024320 (2012).

[10] P. Jachimowicz, M. Kowal, and J. Skalski, Atomic Data and Nuclear Data Tables 138, 101393 (2021).

[11] P. M¨oller, A. J. Sierk, T. Ichikawa and H. Sagawa, At. Data Nucl. Data Tables109 (2016) 1.

[12] W. M. Seif, A. R. Abdulghany, Amira Nasr International Journal of Modern Phys. E 23 2250074 (2022)

[13] P. Marevic, et al., CPC 276 108367 (2022).

Acknowledgments

First of all, I'd like to specially thank my supervisor, Prof. Walaa M. Seif, for giving me this chance to be here with the powerful team in BLTP and for his endless support during the whole time.

I'd also like to express my sincere appreciation and thankfulness to my supervisor, Prof. Nikolai Antonenko. I want to say it has been a pleasure giving me the summer session in the START programme.

I’d also like to extend my sincere gratitude to my supervisor, Prof. Gurgen Adamian.

And finally, last but by no means least, I just had the unique pleasure of meeting you.